

# Structural Coupling of an Arginine Side Chain with the Oxygen-Evolving $Mn_4Ca$ Cluster in Photosystem II As Revealed by Isotope-Edited Fourier Transform Infrared Spectroscopy

Yuichiro Shimada,<sup>†</sup> Hiroyuki Suzuki,<sup>‡</sup> Tohru Tsuchiya,<sup>†</sup> Mamoru Mimuro,<sup>†</sup> and Takumi Noguchi<sup>\*,‡,||</sup>

<sup>†</sup>Graduate School of Human and Environmental Studies, Kyoto University, Kyoto 606-8501, Japan

<sup>‡</sup>Institute of Materials Science, University of Tsukuba, Tsukuba, Ibaraki 305-8573, Japan

<sup>||</sup>Division of Material Science, Graduate School of Science, Nagoya University, Furo-cho, Chikusa-ku, Nagoya 464-8602, Japan

**S** Supporting Information

**ABSTRACT:** Photosynthetic oxygen evolution by plants, algae, and cyanobacteria is performed at the  $Mn_4Ca$  cluster in photosystem II (PSII) by light-driven water oxidation. It has been proposed that CP43-Arg357, which is located in the vicinity of the  $Mn_4Ca$  cluster, plays a key role in the  $O_2$  evolution mechanism; however, direct evidence for its involvement in the reaction has not yet been obtained. In this study, we have for the first time detected the structural coupling of CP43-Arg357 with the  $Mn_4Ca$  cluster by means of isotope-edited Fourier transform infrared (FTIR) spectroscopy. Light-induced FTIR difference spectra upon the  $S_1 \rightarrow S_2$  transition ( $S_2/S_1$  difference spectra) of the  $Mn_4Ca$  cluster were measured using isolated PSII core complexes from *Synechocystis* sp. PCC 6803 cells, where the Arg side chains were labeled with either  $[\eta_{1,2}\text{-}^{15}\text{N}_2]\text{Arg}$  or  $[\zeta\text{-}^{13}\text{C}]\text{Arg}$ . Bands due to Arg side chain vibrations, which were extracted by taking a double difference between the  $S_2/S_1$  spectra of isotope-labeled and unlabeled samples, were found at 1700–1600 and 1700–1550  $\text{cm}^{-1}$  for  $[\eta_{1,2}\text{-}^{15}\text{N}_2]\text{Arg}$ - and  $[\zeta\text{-}^{13}\text{C}]\text{Arg}$ -labeled PSII, respectively. These frequency regions are in good agreement with those of the CN/NH<sub>2</sub> vibrations of a guanidinium group in difference spectra between isotope-labeled and unlabeled Arg in aqueous solutions. The detected Arg bands in the  $S_2/S_1$  difference spectra were attributed to CP43-Arg357, which is the only Arg residue located near the  $Mn_4Ca$  cluster. The presence of relatively high frequency bands arising from unlabeled Arg suggested that the guanidinium  $N_7H_2$  is engaged in strong hydrogen bonding. These results indicate that CP43-Arg357 interacts with the  $Mn_4Ca$  cluster probably through direct hydrogen bonding to a first coordination shell ligand of a redox-active Mn ion. This structural coupling of CP43-Arg357 may play a crucial role in the water oxidation reactions.

Virtually all molecular oxygen comprising 21% of the Earth's atmosphere is generated by photosynthesis via reactions that are catalyzed at the  $Mn_4Ca$  cluster embedded in the photosystem II (PSII) protein complexes of plants, algae, and cyanobacteria. This metal cluster, which is crucial for the global environment and almost all life on Earth, consists of four Mn ions and one Ca ion that are ligated by  $\mu$ -oxo bridges, and carboxylate and

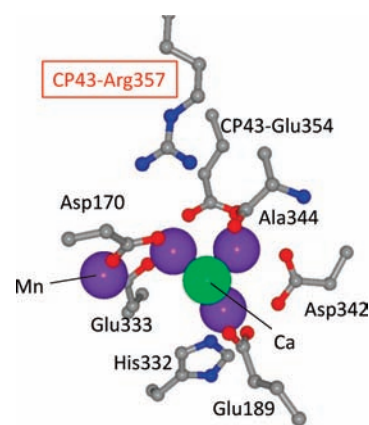


**Figure 1.** Structural relationship of CP43-Arg357 with the Mn cluster in the structural model of PSII by X-ray crystallography.<sup>1b</sup>

imidazole groups from the D1 and CP43 proteins.<sup>1</sup> The  $O_2$  evolution is known to be achieved by four-electron oxidation of two water molecules through a cycle of five intermediates called S states ( $S_0$ – $S_4$ ).<sup>2</sup> However, the detailed mechanism of this reaction, including the catalytic roles of amino acid residues around the  $Mn_4Ca$  cluster, remains largely unknown. It has been proposed that CP43-Arg357, which is located in the vicinity of the  $Mn_4Ca$  cluster (Figure 1), plays a key role in the reaction mechanism.<sup>2c,3</sup> Although site-directed mutagenesis studies have shown the significance of this residue,<sup>4</sup> direct evidence for the involvement of CP43-Arg357 in the  $O_2$ -evolving reaction has yet to be obtained. CP43-Arg357 is not a direct ligand to the  $Mn_4Ca$  cluster and hence has escaped spectroscopic detection. It is thus urgent to develop a method to monitor the changes of the Arg357 side chain during the reaction sequence leading to  $O_2$  evolution. In this study, we have for the first time obtained the signals of the CP43-Arg357 side chain using isotope-edited light-induced FTIR difference spectroscopy<sup>5</sup> and proved that this Arg residue is indeed structurally coupled to the  $Mn_4Ca$  cluster.

The Arg-requiring strain of *Synechocystis* sp. PCC 6803 (designated as  $\Delta\text{ArgH}$ ) was generated by deletion of a putative gene encoding L-argininosuccinate lyase (*slr1133*; *argH*), which is an enzyme involved in Arg biosynthesis, using a strain in which

**Received:** January 7, 2011

**Published:** February 24, 2011

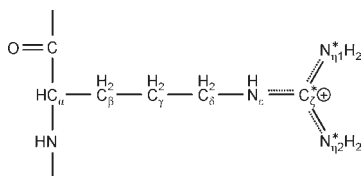


**Figure 2.** Structure of an Arg residue in the guanidinium cation form. Atoms that were labeled with  $^{15}\text{N}$  or  $^{13}\text{C}$  are marked with asterisks.

a His<sub>6</sub>-tag was introduced to the C-terminus of the CP47 protein (designated as WT)<sup>6</sup> as a parental strain (see Supporting Information [SI] for the experimental procedures including the details of construction of the mutant). Isotope labeling of the guanidinium group of Arg in proteins was achieved by culturing  $\Delta\text{ArgH}$  cells in a medium containing 1 mM L-Arg·HCl that is labeled either with  $^{15}\text{N}$  at the  $\eta_{1,2}$ -nitrogens ( $[\eta_{1,2}\text{-}^{15}\text{N}_2]\text{Arg}$ ) or with  $^{13}\text{C}$  at the  $\zeta$ -carbon ( $[\zeta\text{-}^{13}\text{C}]\text{Arg}$ ) instead of unlabeled L-Arg·HCl (see Figure 2 for the positions of isotope-labeled atoms in an Arg side chain). The  $\Delta\text{ArgH}$  cells grew at a rate similar to WT by supplying 1 mM Arg, but did not grow at all in a medium in the absence of Arg (Figure S1D [SI]), indicating that basically all Arg residues were isotope labeled in  $\Delta\text{ArgH}$  cells cultured with  $[\eta_{1,2}\text{-}^{15}\text{N}_2]\text{Arg}$  or  $[\zeta\text{-}^{13}\text{C}]\text{Arg}$ . It was previously reported that no isotopic scrambling to other amino acids occurred in selective isotope labeling of Arg using an Arg auxotrophic strain of *Halobacterium salinarium*.<sup>7</sup> The integrity of the PSII complexes isolated from the  $\Delta\text{ArgH}$  cells was confirmed by absorption and fluorescence spectra, O<sub>2</sub> evolution activities, and SDS-PAGE analysis (see [SI]). Light-induced Fourier transform infrared (FTIR) difference spectra upon the S<sub>1</sub>→S<sub>2</sub> transition (S<sub>2</sub>/S<sub>1</sub> difference spectra) were recorded at 10 °C using hydrated films of PSII complexes as described previously.<sup>8,9</sup>

Figure 3A shows the S<sub>2</sub>/S<sub>1</sub> FTIR difference spectra (1800–1450 cm<sup>-1</sup> region) of unlabeled (black line),  $[\eta_{1,2}\text{-}^{15}\text{N}_2]\text{Arg}$ -labeled (blue line), and  $[\zeta\text{-}^{13}\text{C}]\text{Arg}$ -labeled (red line) PSII core complexes from  $\Delta\text{ArgH}$  cells. The spectrum of unlabeled PSII was virtually identical to that of PSII from WT (data not shown). Bands in this region of the S<sub>2</sub>/S<sub>1</sub> spectra have been assigned mainly to the amide I (1700–1600 cm<sup>-1</sup>; C=O stretches) and amide II (1600–1500 cm<sup>-1</sup>; NH bends + CN stretches) vibrations of backbone amides and the asymmetric COO<sup>-</sup> stretching vibrations of carboxylate groups (1600–1450 cm<sup>-1</sup>).<sup>10</sup> Some spectral changes were clearly observed in the 1700–1600 and 1700–1550 cm<sup>-1</sup> regions upon  $[\eta_{1,2}\text{-}^{15}\text{N}_2]\text{Arg}$  and  $[\zeta\text{-}^{13}\text{C}]\text{Arg}$  labeling, respectively (Figure 3A), whereas no specific changes were observed in the 1550–1100 cm<sup>-1</sup> region that includes the prominent symmetric COO<sup>-</sup> bands (1450–1350 cm<sup>-1</sup>) (spectra in the 1800–1100 cm<sup>-1</sup> region are shown in Figures S5 and S6 in Supporting Information [SI]). It should be noted that the 1185/1174 cm<sup>-1</sup> bands, which were tentatively assigned to Arg vibrations in the previous FTIR study by Kimura et al.<sup>11</sup> using global  $^{15}\text{N}$  labeling (1186/1178 cm<sup>-1</sup> bands in their spectra), were sensitive neither to  $[\eta_{1,2}\text{-}^{15}\text{N}_2]\text{Arg}$  nor to  $[\zeta\text{-}^{13}\text{C}]\text{Arg}$  labeling, dismissing this assignment.

Figure 3B (solid lines) shows FTIR spectra of unlabeled and isotope-labeled Arg·HCl in aqueous solutions. In the spectrum of unlabeled Arg (black solid line), the 1667 and 1632 cm<sup>-1</sup> bands are attributed to the vibrations of the guanidinium group of Arg,<sup>12–14</sup> while the 1596 and 1522 cm<sup>-1</sup> bands arise from the COO<sup>-</sup> asymmetric stretch and the NH<sub>3</sub><sup>+</sup> symmetric deformation, respectively, of an  $\alpha$ -amino acid group.<sup>14</sup> The NH<sub>3</sub><sup>+</sup> asymmetric

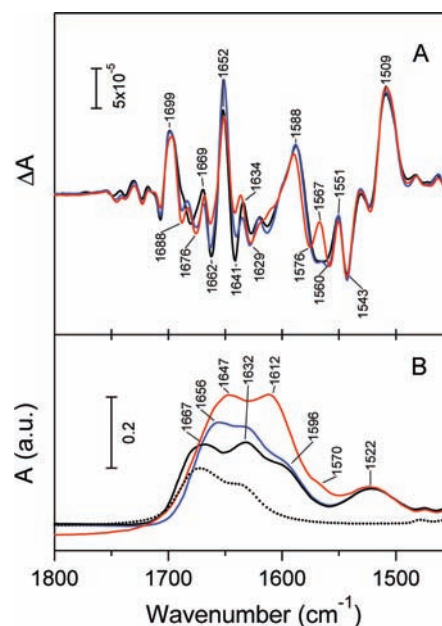


**Figure 3.** (A) S<sub>2</sub>/S<sub>1</sub> FTIR difference spectra of unlabeled (black line),  $[\eta_{1,2}\text{-}^{15}\text{N}_2]\text{Arg}$ -labeled (blue line), and  $[\zeta\text{-}^{13}\text{C}]\text{Arg}$ -labeled (red line) PSII core complexes. Isotope-labeled spectra were normalized to the unlabeled one based on the symmetric COO<sup>-</sup> stretching region of 1450–1350 cm<sup>-1</sup> (Figures S5 and S6 [SI]). (B) FTIR spectra of unlabeled (black solid line),  $\eta_{1,2}\text{-}^{15}\text{N}_2$ -labeled (blue line), and  $\zeta\text{-}^{13}\text{C}$ -labeled (red line) Arg HCl, and ethylguanidine HCl (black dotted line) in aqueous solutions. Arg spectra were normalized on the intensity of the NH<sub>3</sub><sup>+</sup> band at 1522 cm<sup>-1</sup>.

deformation also has a band around 1630 cm<sup>-1</sup> overlapping the guanidinium band.<sup>14</sup> The above assignment of the guanidinium group is supported by the FTIR spectrum of ethylguanidine·HCl (black dotted line) showing bands at 1672 and 1636 cm<sup>-1</sup>. These two bands actually consist of three vibrational modes of the CN stretches coupled with the NH<sub>2</sub> bends of the guanidinium group.<sup>15</sup> Upon  $\eta_{1,2}\text{-}^{15}\text{N}_2$  labeling of the Arg guanidinium group (blue line), the band at 1667 cm<sup>-1</sup> was downshifted to 1656 cm<sup>-1</sup>, while upon  $\zeta\text{-}^{13}\text{C}$  labeling (red line), the bands at 1667 and 1632 cm<sup>-1</sup> seemed to downshift to 1647 and 1612 cm<sup>-1</sup> with additional weak band at ~1570 cm<sup>-1</sup>.

These isotope-induced spectral changes are more clearly revealed in unlabeled–minus–isotope-labeled difference spectra (Figure 4). An S<sub>2</sub>/S<sub>1</sub> double difference spectrum by  $[\eta_{1,2}\text{-}^{15}\text{N}_2]\text{Arg}$  labeling of PSII (Figure 4a) showed peaks at 1689, 1682, 1673, 1650, and 1632 cm<sup>-1</sup>, while Arg in aqueous solution (Figure 4b) showed bands at 1686, 1653, and 1623 cm<sup>-1</sup> by the same labeling. Also,  $[\zeta\text{-}^{13}\text{C}]\text{Arg}$  labeling of PSII (Figure 4c) provided peaks at 1689, 1682, 1674, 1661, 1654, 1641, 1631, 1611, 1581, and 1567 cm<sup>-1</sup> in a double difference spectrum, while  $\zeta\text{-}^{13}\text{C}$ -labeled Arg in solution (Figure 4d) showed bands at 1685, 1648, 1609, and 1571 cm<sup>-1</sup>. Thus, the frequency regions where the signals appeared in the S<sub>2</sub>/S<sub>1</sub> double difference spectra are in good agreement with those of corresponding difference spectra of Arg in water (1690–1620 and 1690–1565 cm<sup>-1</sup> for  $\eta_{1,2}\text{-}^{15}\text{N}_2$  and  $\zeta\text{-}^{13}\text{C}$  labeling, respectively). In particular, the wider frequency range in  $\zeta\text{-}^{13}\text{C}$  than in  $\eta_{1,2}\text{-}^{15}\text{N}_2$  labeling, representing a larger  $^{13}\text{C}$  downshift than a  $^{15}\text{N}$  downshift, is well reproduced in the S<sub>2</sub>/S<sub>1</sub> double difference spectra. These results indicate that we indeed detected the Arg signals that are involved in the S<sub>2</sub>/S<sub>1</sub> difference spectrum.

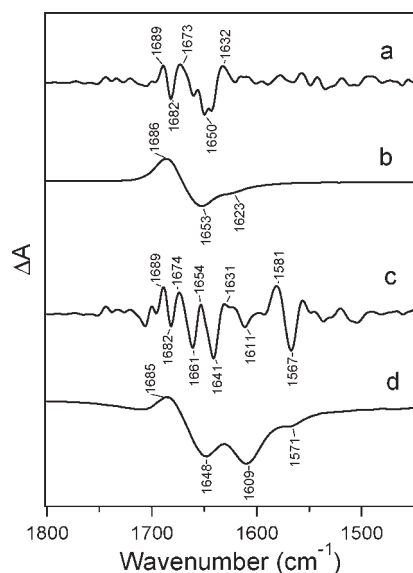


**Figure 4.** Unlabeled–minus-isotope-labeled difference spectra. (a) A double difference spectrum between the  $S_2/S_1$  difference spectra of  $[\eta_{1,2}\text{-}^{15}\text{N}_2]$ -Arg-labeled and unlabeled PSII. (b) A difference spectrum between  $\eta_{1,2}\text{-}^{15}\text{N}_2$ -labeled and unlabeled Arg in aqueous solution. (c) A double difference spectrum between the  $S_2/S_1$  difference spectra of  $[\xi\text{-}^{13}\text{C}]$ -Arg-labeled and unlabeled PSII. (d) A difference spectrum between  $\xi\text{-}^{13}\text{C}$ -labeled and unlabeled Arg in aqueous solution.

The peaks at 1689(+)/1682(−)  $\text{cm}^{-1}$ , which were commonly observed in both of the double difference spectra of PSII (Figure 4a, c), correspond to the  $\sim 1685$ (+)  $\text{cm}^{-1}$  band in the difference spectra of Arg in solution (Figure 4b, d) and hence are assignable to the highest-frequency CN/NH<sub>2</sub> vibration of unlabeled Arg in the  $S_2/S_1$  difference spectrum. Since stronger hydrogen bonding tends to upshift the frequency of this CN/NH<sub>2</sub> vibration,<sup>12,13</sup> the relatively high frequencies of the 1689(+)/1682(−)  $\text{cm}^{-1}$  peaks comparable to the frequency of Arg in water indicate that the guanidinium group is engaged in strong hydrogen bonding. Also, the prominent differential signal at 1581(+)/1567(−)  $\text{cm}^{-1}$  in the double difference spectrum by  $[\xi\text{-}^{13}\text{C}]$ -Arg labeling (Figure 4c) corresponds to the 1571(−)  $\text{cm}^{-1}$  band in the unlabeled–minus- $\xi\text{-}^{13}\text{C}$ -labeled Arg in aqueous solution (Figure 4d). Hence, the origin of the 1581/1567  $\text{cm}^{-1}$  signal is the lower-frequency CN/NH<sub>2</sub> vibration of the  $\xi\text{-}^{13}\text{C}$ -guanidinium group. The much stronger intensity of this signal than the intensity of the 1571  $\text{cm}^{-1}$  band in solution could indicate a specific conformation of hydrogen bonding interactions of the guanidinium group, although further investigations using theoretical calculations and model compound measurements are necessary to understand the structural implications. It should be noted that since the amide I bands around 1650  $\text{cm}^{-1}$  in the  $S_2/S_1$  spectrum are rather sensitive to sample conditions (e.g., hydration extent), the peaks around 1650  $\text{cm}^{-1}$  in the double difference spectra (Figure 4a, c) could be disturbed to some extent by such variable amide I changes.

It has been shown that a deprotonated guanidine group has a band at 1600–1550  $\text{cm}^{-1}$ ,<sup>13,16</sup> the frequency region much lower than that of a protonated guanidinium group (1690–1630  $\text{cm}^{-1}$ ; Figure 3B, dotted line). However, no meaningful bands were found in this low frequency region in the unlabeled–minus- $[\eta_{1,2}\text{-}^{15}\text{N}_2]$ -Arg-labeled double difference spectrum (Figure 3a). (Weak features in the region lower than 1600  $\text{cm}^{-1}$  were not reproducible

and hence ascribed to noise.) It is thus concluded that the Arg side chain detected by FTIR is basically in a protonated state in both the  $S_1$  and  $S_2$  states, although the presence of a deprotonated state in a minor fraction of centers cannot be excluded.

The above results definitely proved that there is an Arg side chain that is structurally coupled with the Mn<sub>4</sub>Ca cluster. The presence of about twice the number of bands in the  $S_2/S_1$  double difference spectra (Figure 4a, c) compared with the corresponding difference spectra of Arg in solutions (Figure 4b, d) is consistent with the idea that only one Arg side chain is involved in the coupling, because a single vibration should provide two peaks in the  $S_2/S_1$  difference spectra. CP43-Arg357 is located in the vicinity of the Mn<sub>4</sub>Ca cluster (the shortest distance between the N<sub>η</sub> atom and the Mn ion is 4.4 Å in the X-ray structure<sup>1b</sup>), and it is the only Arg side chain within 10 Å from the Mn<sub>4</sub>Ca cluster. Thus, CP43-Arg357 is the most probable candidate for the Arg residue responsible for the observed structural coupling. The presence of this coupling, strong hydrogen bonding of the N<sub>η</sub>H<sub>2</sub> (see above), and the distance of 4–5 Å from the Mn<sub>4</sub>Ca cluster are all consistent with view that CP43-Arg357 directly interacts with a first coordination shell ligand of the Mn<sub>4</sub>Ca cluster.<sup>17</sup>

In conclusion, we have succeeded in detecting the structural coupling of CP43-Arg357 with the Mn<sub>4</sub>Ca cluster by means of light-induced FTIR difference measurements in combination with selective isotope labeling of Arg side chains. Because of the strong coupling between Arg and the Mn<sub>4</sub>Ca cluster, it is highly likely that this residue plays crucial roles in the O<sub>2</sub>-evolving reactions such as by upshifting the redox potential of the Mn<sub>4</sub>Ca cluster by a positive charge of Arg to facilitate water oxidation and formation of the reaction field of substrate water by a hydrogen-bond network around the Mn<sub>4</sub>Ca cluster. The significance of such a hydrogen-bond network in the O–O bond formation has been pointed out previously.<sup>2c</sup> It is also possible that CP43-Arg357 is deprotonated upon Y<sub>Z</sub> oxidation or in higher S states, functioning as a proton acceptor as previously proposed.<sup>2c,3</sup> Further FTIR measurements to monitor the Arg reactions during the S-state cycle and determining clear criteria to interpret the Arg bands will provide important information to understand the molecular mechanism of photosynthetic O<sub>2</sub> evolution.

## ■ ASSOCIATED CONTENT

**S Supporting Information.** The details of experimental procedures, characterization of the  $\Delta$ ArgH strain and isolated PSII complexes, and FTIR spectra in the 1800–1100  $\text{cm}^{-1}$  region. This material is available free of charge via the Internet at <http://pubs.acs.org>.

## ■ AUTHOR INFORMATION

**Corresponding Author**  
tnoguchi@bio.phys.nagoya-u.ac.jp

## ■ ACKNOWLEDGMENT

This study was supported by the Grants-in-Aid for Scientific Research from the Ministry of Education, Culture, Sports, Science and Technology (17GS0314 to M.M. and T.N., 22370017 to M.M., and 21108506 and 21370063 to T.N.) and Grant-in-Aid for JSPS fellows (224953 to H.S.). Y.S., H.S., T.T.,

and T. N. dedicate this work to their co-author, Mamoru Mimuro (deceased, February 8, 2011).

## REFERENCES

- (1) (a) Ferreira, K. N.; Iverson, T. M.; Maghlaoui, K.; Barber, J.; Iwata, S. *Science* **2004**, *303*, 1831–1838. (b) Guskov, A.; Kern, J.; Gabdulkhakov, A.; Broser, M.; Zouni, A.; Saenger, W. *Nat. Struct. Mol. Biol.* **2009**, *16*, 334–342. (c) Kawakami, K.; Umena, Y.; Kamiya, N.; Shen, J.-R. *Proc. Natl. Acad. Sci. U.S.A.* **2009**, *106*, 8567–8572. (d) Yano, J.; Kern, J.; Sauer, K.; Latimer, M. J.; Pushkar, Y.; Biesiadka, J.; Loll, B.; Saenger, W.; Messinger, J.; Zouni, A.; Yachandra, V. K. *Science* **2006**, *314*, 821–825.
- (2) (a) Debus, R. J. *Biochim. Biophys. Acta* **1992**, *1102*, 269–352. (b) Hillier, W.; Messinger, J. *Photosystem II: The Light-Driven Water: Plastoquinone Oxidoreductase*; Wydrzynski, T., Satoh, K., Eds.; Springer: Dordrecht, The Netherlands, 2005; pp 567–608. (c) McEvoy, J. P.; Brudvig, G. W. *Chem. Rev.* **2006**, *106*, 4455–4483. (d) Renger, G. *Photosynth. Res.* **2007**, *92*, 407–425. (e) Renger, G.; Renger, T. *Photosynth. Res.* **2008**, *98*, 53–80.
- (3) Haumann, M.; Liebisch, P.; Müller, C.; Barra, M.; Grabolle, M.; Dau, H. *Science* **2005**, *310*, 1019–1021.
- (4) (a) Knoepfle, N.; Bricker, T. M.; Putnam-Evans, C. *Biochemistry* **1999**, *38*, 1582–1588. (b) Hwang, H. J.; Dilbeck, P.; Debus, R. J.; Burnap, R. L. *Biochemistry* **2007**, *46*, 11987–11997. (c) Ananyev, G.; Nguyen, T.; Putnam-Evans, C.; Dismukes, G. C. *Photochem. Photobiol. Sci.* **2005**, *4*, 991–998.
- (5) (a) Noguchi, T. *Photosynth. Res.* **2007**, *91*, 59–69. (b) Noguchi, T. *Coord. Chem. Rev.* **2008**, *252*, 336–346. (c) Debus, R. J. *Coord. Chem. Rev.* **2008**, *252*, 244–258. (d) Berthomieu, C.; Hienerwadel, R. *Photosynth. Res.* **2009**, *101*, 157–170.
- (6) Mimuro, M.; Akimoto, S.; Tomo, T.; Yokono, M.; Miyashita, H.; Tsuchiya, T. *Biochim. Biophys. Acta* **2007**, *1767*, 327–334.
- (7) Petkova, A. T.; Hu, J. G.; Bizounok, M.; Simpson, M.; Griffin, R. G.; Herzfeld, J. *Biochemistry* **1999**, *38*, 1562–1572.
- (8) Noguchi, T.; Sugiura, M. *Biochemistry* **2002**, *41*, 2322–2330.
- (9) Shimada, Y.; Suzuki, H.; Tsuchiya, T.; Tomo, T.; Noguchi, T.; Mimuro, M. *Biochemistry* **2009**, *48*, 6095–6103.
- (10) (a) Noguchi, T.; Sugiura, M. *Biochemistry* **2003**, *42*, 6035–6042. (b) Kimura, Y.; Mizusawa, N.; Ishii, A.; Yamanari, T.; Ono, T. *Biochemistry* **2003**, *42*, 13170–13177.
- (11) Kimura, Y.; Mizusawa, N.; Ishii, A.; Ono, T. *Biochemistry* **2005**, *44*, 16072–16078.
- (12) Braiman, M. S.; Walter, T. J.; Briercheck, D. M. *Biochemistry* **1994**, *33*, 1629–1635.
- (13) Braiman, M. S.; Briercheck, D. M.; Kriger, K. M. *J. Phys. Chem. B* **1999**, *103*, 4744–4750.
- (14) Venyaminov, S. Y.; Kalnin, N. N. *Biopolymers* **1990**, *30*, 1243–1257.
- (15) Rak, J.; Skurski, P.; Simons, J.; Gutowski, M. *J. Am. Chem. Soc.* **2001**, *123*, 11695–11707.
- (16) Xiao, Y. W.; Hutson, M. S.; Belenky, M.; Herzfeld, J.; Braiman, M. S. *Biochemistry* **2004**, *43*, 12809–12818.
- (17) This conclusion from FTIR is consistent with the very recent X-ray structure at 1.9 Å resolution by Shen and co-workers (the 15th International Congress of Photosynthesis in Beijing, PS6.5), in which the N<sub>7</sub> of CP43-Arg357 is located in a hydrogen bond distance from the  $\mu$ -oxo ligand to the Mn<sub>4</sub>Ca cluster.